Free Radical Biology and Medicine 87 (2015) 263–273

Contents lists available at ScienceDirect

Free Radical Biology and Medicine

journal homepage: www.elsevier.com/locate/freeradbiomed

Monoamine oxidase-A is an important source of oxidative stress and promotes cardiac dysfunction, apoptosis, and fibrosis in diabetic cardiomyopathy

Prachi Umbarkar [a], Sarojini Singh [a,1], Silpa Arkat [a,1], S.L. Bodhankar [b], Sathiyanarayanan Lohidasan [c], Sandhya L. Sitasawad [a,*]

[a] National Centre for Cell Science, NCCS Complex, S.P. Pune University, Ganeshkhind, Pune 411007, Maharashtra, India
[b] Department of Pharmacology, Poona College of Pharmacy, Bharati Vidyapeeth Deemed University, Erandwane, Pune, India
[c] Department of Pharmaceutical Chemistry, Poona College of Pharmacy, Bharati Vidyapeeth Deemed University, Erandwane, Pune, India

ARTICLE INFO

Article history:
Received 6 February 2015
Received in revised form
22 May 2015
Accepted 9 June 2015
Available online 26 June 2015

Keywords:
Diabetic cardiomyopathy
Monoamine oxidase A
Oxidative stress
Cardiac dysfunction
Apoptosis
Free radicals

ABSTRACT

Oxidative stress is closely associated with the pathophysiology of diabetic cardiomyopathy (DCM). The mitochondrial flavoenzyme monoamine oxidase A (MAO-A) is an important source of oxidative stress in the myocardium. We sought to determine whether MAO-A plays a major role in modulating DCM. Diabetes was induced in Wistar rats by single intraperitoneal injection of streptozotocin (STZ). To investigate the role of MAO-A in the development of pathophysiological features of DCM, hyperglycemic and age-matched control rats were treated with or without the MAO-A-specific inhibitor clorgyline (CLG) at 1 mg/kg/day for 8 weeks. Diabetes upregulated MAO-A activity; elevated markers of oxidative stress such as cardiac lipid peroxidation, superoxide dismutase activity, and UCP3 protein expression; enhanced apoptotic cell death; and increased fibrosis. All these parameters were significantly attenuated by CLG treatment. In addition, treatment with CLG substantially prevented diabetes-induced cardiac contractile dysfunction as evidenced by decreased QRS, QT, and corrected QT intervals, measured by ECG, and LV systolic and LV end-diastolic pressure measured by microtip pressure transducer. These beneficial effects of CLG were seen despite the persistent hyperglycemic and hyperlipidemic environments in STZ-induced experimental diabetes. In summary, this study provides strong evidence that MAO-A is an important source of oxidative stress in the heart and that MAO-A-derived reactive oxygen species contribute to DCM.

Diabetic cardiomyopathy (DCM) carries a substantial risk concerning the subsequent development of heart failure and increased mortality in diabetic patients [1]. It is characterized by early diastolic dysfunction, accompanied by cardiomyocyte apoptosis, compensatory hypertrophy, and reparative fibrosis [2]. Although the features of diabetic cardiomyopathy have been well identified, comprehensive understanding of the mechanisms underlying the myocardial remodeling process is urgently needed.

Oxidative stress has been widely implicated in diabetes and its many complications [3]. The heart is particularly susceptible to oxidative damage, as it possesses lower levels of free radical scavengers in comparison to other organs [4]. Increased levels of cardiac lipid peroxidation and activity of antioxidant enzymes such as catalase and superoxide dismutase seem to be relevant with respect to oxidative stress in diabetes [5,6]. Experimental models have allowed a better understanding of how oxidative stress causes myocardial apoptosis and activates a series of cardiac remodeling responses, leading to morphological and functional abnormalities and eventually to cardiomyopathy [7]. In vivo studies demonstrated that diabetes-induced cardiac remodeling and dysfunction can be reduced by targeting ROS with oral or systemic antioxidant administration [5,8]. However, the precise sources of ROS in the myocardium under diabetic conditions are unknown.

Monoamine oxidases (MAOs) are mitochondrial flavoproteins responsible for oxidation of monoamines. During this process they generate H_2O_2 and reactive aldehydes as by-products. Based on

Abbreviations: MAO, monoamine oxidase; DCM, diabetic cardiomyopathy; I/R, ischemia/reperfusion; STZ, streptozotocin; CLG, clorgyline; HW, heart weight; BW, body weight; NE, norepinephrine; DHPG, dihydroxyphenylglycol; 5-HT, 5-hydroxytryptamine; ECG, electrocardiography; MABP, mean arterial blood pressure; LVSP, left-ventricular systolic pressure; LVEDP, left-ventricular end-diastolic pressure; ROS, reactive oxygen species; MDA, malondialdehyde; Prx, peroxiredoxin; UCP3, uncoupling protein 3; GPx, glutathione peroxidase; COX IV, cytochrome oxidase subunit IV; TUNEL, terminal deoxynucleotidyl transferase-mediated dUTP nick-end labeling

* Corresponding author. Fax: +91 20 25692259.
E-mail address: ssitaswad@nccs.res.in (S.L. Sitasawad).
[1] These authors contributed equally to this work.

http://dx.doi.org/10.1016/j.freeradbiomed.2015.06.025

substrate specificity and inhibitor sensitivity, two isoforms of MAO have been identified, MAO-A and MAO B. However, MAO-A appears to be the predominant isoform in the myocardium of several species [9]. Recent findings demonstrate that pharmacological or genetic inhibition of MAO-A prevents maladaptive remodeling and left-ventricular dysfunction in mouse hearts subjected to pressure overload [10]. Overexpression of MAO-A in mouse heart causes oxidative stress-mediated mitochondrial damage and cardiomyocyte necrosis, leading to ventricular dysfunction [11]. Moreover the important role of MAO as a relevant source of ROS in ischemia/reperfusion (I/R) injury was demonstrated both ex vivo [12] and in vivo [13,14]. Yet the involvement of MAO-A in diabetic cardiomyopathy is not defined.

Therefore, we aimed to investigate whether MAO-A can potentially be a relevant source of ROS and contribute to the development of diabetic cardiomyopathy. In the current study, we found that MAO-A activity but not protein expression was significantly upregulated in the myocardium of diabetic rats. Further we have shown that inhibition of myocardial MAO-A activity with a MAO-A specific inhibitor, CLG, reduced cardiac oxidative stress, apoptosis, and fibrosis, thus preventing cardiac dysfunction in streptozotocin (STZ)-induced diabetic rats.

1. Materials and methods

1.1. Animals and treatments

All animal research was approved by the Institutional Animal Ethics Committee at the National Centre for Cell Science (Pune, India). Male Wistar rats were housed in a temperature-controlled room under a 12-h light/dark circadian cycle with access to water and food ad libitum. At 6–8 weeks of age, rats were intraperitoneally (ip) administered a single dose of STZ (Sigma–Aldrich, St. Louis, MO, USA) at 55 mg/kg BW, dissolved in 0.1 mol/L citrate buffer, pH 4.5. An equivalent volume of citrate buffer was administered to the vehicle control group. On day 3 after STZ treatment, whole-blood glucose obtained from the rat tail vein was monitored using a glucometer (Contour; Bayer, USA). Streptozotocin-treated rats with fasting blood glucose higher than 12 mmol/L were considered diabetic. The rats were allocated into the following groups: rats that received only vehicle (control, $n = 6$), rats treated with CLG (CLG, $n = 6$), STZ-induced diabetic rats (STZ, $n = 9$), and diabetic rats treated with CLG (STZ + CLG, $n = 8$). CLG was administered using saline as vehicle (1 mg/kg/day, ip) on 4th day after the initial STZ/citrate buffer injection for 8 weeks.

1.2. Assessment of electrocardiographic and hemodynamic changes and left-ventricular contractile function

At the end of 8 weeks, the rats were weighed and anesthetized using urethane (1 g/kg/ BW, ip). Urethane was selected as an anesthetic agent as its single dose induces long-term anesthesia and analgesia with minimal cardiovascular and respiratory system depression [15]. The right carotid artery was cannulated with a microtip pressure transducer (SPR-320; Millar Instruments) connected to an eight-channel PowerLab instrument via a bridge amplifier (ADInstruments, Colorado Springs, CO, USA). The pressure-tip transducer catheter was then advanced into the left ventricle for the evaluation of ventricular pressures. LV systolic and end-diastolic pressures and the maximum rate of LV systolic pressure rise and fall ($\pm dp/dt$) were monitored and recorded using Chart 5.5 (ADInstruments).

ECG leads were recorded with surface electrodes (ADInstruments). The mean value for each rat was obtained from four values consisting of four consecutive cardiac cycles using LabChart software (ADInstruments). Corrected QT (QTc) intervals were analyzed for an evaluation independent of heart rate. QTc was calculated with mean values and the Bazett formula (QTc = QT interval/$\sqrt{}$(RR interval) [16].

1.3. Collection of blood, serum, and hearts from rats

After the hemodynamic measurements were recorded, hearts were excised surgically and blood was collected. After the removal of heart, it was washed with chilled phosphate-buffered saline (PBS) to clear out blood. The ventricular portions of the heart were removed and snap-frozen in liquid nitrogen for further experiments. For isolation of serum, the blood was allowed to clot at room temperature for 10 to 15 min and then centrifuged for 10 min at 3000*g;* clear serum was obtained and stored at −80°C until use.

1.4. Blood analysis

Serum levels of total cholesterol, low-density lipoprotein (LDL), high-density lipoprotein (HDL), and troponin I levels were analyzed using appropriate kits on an RA-50 semiautoanalyzer by well-standardized methods. Serum insulin levels were measured by enzyme-linked immunosorbent assay (Mercodia AB, Sweden).

1.5. Liver function tests

Quantitative estimation of serum glutamate pyruvate transaminase (SGPT) and serum glutamate oxaloacetate transaminase (SGOT) was done using a specific kit (Erba Diagnostics Mannheim GmbH, Germany) on an RA-50 semiautoanalyzer by well-standardized methods [17].

1.6. Measurement of myocardial lipid peroxidation and antioxidant enzyme activity

To assess myocardial lipid peroxidation, myocardial 4-hydroxynonenal (4-HNE) and malondialdehyde (MDA) levels were examined.

Immunofluorescence staining was carried out for 4-HNE. Hearts were embedded in Tissue-Plus OCT compound (Fisher Scientific, USA). Cryosections, 8 μm in thickness, were cut with a cryostat (Shandon Cryotome; SME Cryostat) at −20°C and transferred onto Superfrost Plus Gold microscope slides (Fisher Scientific). Frozen heart sections were fixed in 3.7% paraformaldehyde. After nonspecific binding was blocked with 3% bovine serum albumin, the sections were incubated with a rabbit polyclonal anti-4-HNE antibody (Alpha Diagnostic International, USA), followed by Alexa Fluor 594-conjugated goat anti-rabbit IgG antibody (Invitrogen, USA). Slides were then mounted and imaged in an Olympus FluoView FV10i confocal laser scanning microscope. For negative-control experiments, primary antibody was omitted. Images were analyzed using computer-assisted image analysis systems (ImageJ; National Institutes of Health (NIH)).

Quantification of MDA as a dithiobarbituric acid adduct was done using an HPLC–Vis method as described previously [18].

The levels of superoxide dismutase (SOD), catalase, and glutathione peroxidase (GPx) enzyme activities were measured using a SOD Assay Kit-WST (Sigma), Amplex Red Catalase Assay Kit (Invitrogen), and Glutathione Peroxidase Activity Kit (Enzo Life Sciences), respectively, according to the manufacturer's instructions. Enzyme activities were normalized to protein concentration in the samples.

Table 1
Physiological parameters of the experimental animals

	Control	CLG	STZ	STZ + CLG
Body weight (g)	334.71 ± 6.71	338.17 ± 2.95	262.13 ± 5**	215.86 ± 11.44
HW/BW (mg/g)	2.93 ± 0.08	3.33 ± 0.15	3.61 ± 0.12**	3.91 ± 0.12
Serum insulin (ng/ml)	0.30 ± 0.08	0.49 ± 0.08	0.16 ± 0.03**	0.15 ± 0.01
Blood glucose (mg/dl)	95.29 ± 7.09	88.83 ± 12.91	541.60 ± 13.85***	550.71 ± 9.57
Total cholesterol (mg/dl)	35.00 ± 1.93	49.17 ± 1.64	51.56 ± 3.50***	49.14 ± 1.22
HDL/LDL ratio	0.479 ± 0.08	0.362 ± 0.03	0.328 ± 0.01*	0.346 ± 0.01
Liver function test				
SGPT (IU/L)	52.83 ± 4.17	50.20 ± 3.15	88.75 ± 8.93*	97.29 ± 7.92
SGOT (IU/L)	115.80 ± 3.40	120.67 ± 7.01	157.17 ± 5.26*	152.13 ± 17.13
Troponin I (biomarker of myocardial injury; ng/ml)	0.09 ± 0.03	0.05 ± 0.02	0.31 ± 0.06***	0.09 ± 0.03#

All values are given as mean ± SE (n = 6–8/group).
* $p < 0.05$ vs control group.
** $p < 0.01$ vs control group.
*** $p < 0.001$ vs control group.
# $p < 0.05$ vs STZ group.

Table 2
Hemodynamic and ECG interval measurements of the experimental animals

	Control	CLG	STZ	STZ + CLG
ECG parameters				
Heart rate (bpm)	239.88 ± 8.71	305.41 ± 12.75	199.15 ± 7.97*	231.58 ± 11.90
QRS interval (ms)	27.78 ± 0.25	33.50 ± 0.58	35.91 ± 0.28***	33.50 ± 1.12#
QT interval (ms)	139.58 ± 5.12	110.90 ± 1.59	177.27 ± 7.59**	152.46 ± 5.41#
QTc (ms)	203.70 ± 7.05	171.20 ± 4.09	231.36 ± 3.47*	204.03 ± 5.21#
Hemodynamic parameters				
MABP (mm Hg)	72.44 ± 2.91	78.54 ± 4.84	98.07 ± 4.57*	62.96 ± 7.56###
Systolic duration (s)	0.088 ± 0.004	0.076 ± 0.003	0.111 ± 0.006**	0.111 ± 0.007 (ns)
Diastolic duration (s)	0.165 ± 0.006	0.125 ± 0.008	0.193 ± 0.008*	0.151 ± 0.009#
Contractility index (1/s)	10.43 ± 0.60	9.41 ± 0.37	7.06 ± 0.45*	10.15 ± 1.07#

bpm, beats per minute; MABP, mean arterial blood pressure. All values are given as the mean ± SE (n = 4–8/group).
* $p < 0.05$ vs control group.
** $p < 0.01$ vs control group.
*** $p < 0.001$ vs control group.
# $p < 0.05$ vs STZ group.
$p < 0.001$ vs STZ group.

1.7. HPLC measures for catecholamine levels

Ventricular tissues (50 mg) were homogenized on ice in 0.1 M perchloric acid, 0.3 mM EDTA, and 10^{-7} M ascorbic acid. Homogenates were centrifuged at 4 °C, 12,000 rpm, for 5 min. The supernatants were filtered using 0.22-μm nylon disposable syringe filters and stored at −80 °C until analyzed. Dihydroxybenzylamine was used as an internal standard. Norepinephrine (NE) and dihydroxyphenylglycol (DHPG) were determined by HPLC as described previously [19].

1.8. Determination of MAO-A activity assay

MAO-A activity was determined using the Amplex Red Monoamine Oxidase Assay Kit from Invitrogen. The assay was optimized to measure MAO-A activity in heart tissue homogenates using 5-hydroxytryptamine (5-HT) as the enzymatic substrate. Forty micrograms of heart tissue lysates were incubated for 1 h at 37 °C with 2 mM 5-HT, 400 μmol Amplex red, and 2 U/ml horseradish peroxidase solution. The fluorescence was measured in a fluorescence microplate reader (Synergy HT; BioTek, USA) using excitation in the range of 530/25 nm and emission detection at 590/20 nm. Resorufin was used to prepare a standard curve. MAO activity was expressed as micromoles of resorufin formed per milligram of protein per hour [20,21].

1.9. Estimation of caspase 3 and caspase 9 activity

Tissue homogenates were centrifuged (10,000 g at 4 °C, 10 min) and pellets were lysed in an ice-cold cell lysis buffer (50 mM HEPES, pH 7.4, 0.1% CHAPS, 100 mM NaCl, 1 mM dithiothreitol (DTT), and 0.1 mM EDTA). The assay was carried out in a 96-well plate with each well containing 10 μl cell lysate, 80 μl of assay buffer (50 mM HEPES, pH 7.4, 0.1% CHAPS, 100 mM NaCl, 10 mM DTT, 0.1 mM EDTA, and 10% glycerol), and 10 μl of caspase colorimetric substrate (2 mM). For measurement of caspase 3 and 9 activity, caspase 3 colorimetric substrate (Ac-DEVD-pNA; Calbiochem) and caspase 9 colorimetric substrate (Ac-LEHD-pNA; Sigma) were used, respectively. The plate was incubated at 37 °C for 1 h. Cleavage of the chromophore pNA from the substrate molecule was monitored at 405 nm. Caspase 3 and 9 activities were expressed as picomoles of pNA released per microgram of protein per minute [22].

1.10. Histological examination of myocardial tissues

Heart ventricular portions were fixed in 10% neutral-buffered formalin. The specimens were embedded in paraffin and cut into 5-μm sections. Morphological changes were examined. Images of hematoxylin and eosin (H&E)-stained sections were captured. Interstitial and perivascular fibrosis was evaluated by Picrosirius red staining. Sections were stained with 0.1% Sirius red F3BA and 0.25% fast green FCF for the collagen accumulation and observed under a microscope (SONY, DSC-w530) at 200× magnification. Photomicrographs of the sections were evaluated for collagen fractions using computer-assisted image analysis systems (ImageJ; NIH) as described in a previous study [23].

1.11. Tunel assay

For terminal deoxynucleotidyl transferase-mediated dUTP nick-end labeling (TUNEL) assay, an in situ cell death detection kit (Roche GmbH, Germany) was used according to the manufacturer's instructions. Briefly, the slides were deparaffinized and rehydrated using xylene and ethanol gradings and permeabilized

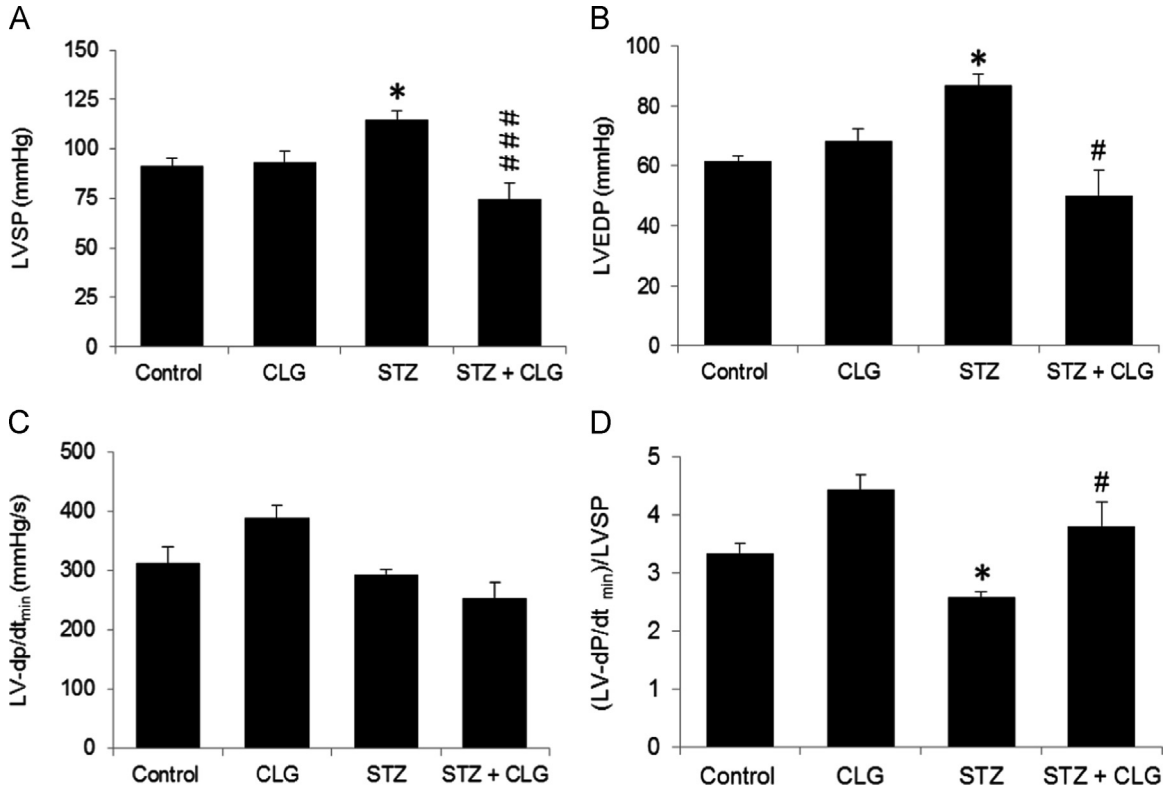

Fig. 1. MAO-A inhibition prevents diabetes-induced cardiac dysfunction. (A) Left-ventricular systolic pressure, (B) left-ventricular end-diastolic pressure, (C) LV $-dp/dt_{min}$ and (D) (LV $-dP/dt_{min}$)/LVSP. All values are given as the mean ± SE ($n = 5$/group); $^{*}p < 0.05$ vs control group; $^{\#}p < 0.05$, $^{\#\#\#}p < 0.001$ vs STZ group.

usingProteinase K solution, and incubated with the reaction mixture containing TdT and fluorescein-labeled dUTP for 1 h at 37 °C. Images were captured with a confocal laser scanning microscope (Zeiss LSM510). For a negative control, TdT was omitted from the reaction mixture. TUNEL-positive and 4′,6-diamidino-2-phenylindole-stained nuclei were counted using the ImageJ software (version 1.43r; NIH). At least 500 cells were counted in each field [22].

1.12. Western blot analysis

Heart tissues were rinsed with cold PBS and then homogenized in RIPA buffer (50 mM Tris–HCl, pH 7.5, 150 mM NaCl, 1.0% NP-40, 1.0% Triton X-100, 0.1% SDS, 1% sodium deoxycholate, 10% glycerol, 1 mM EDTA, and protease inhibitor cocktail; Roche). Protein concentrations were determined by Bradford assay (Bio-Rad protein assay kit). Equal amount of proteins (40 μg) were denatured in SDS–PAGE sample buffer, resolved by SDS–PAGE, and transferred to a polyvinylidene difluoride membrane followed by blocking of the membrane with 5% nonfat milk powder (w/v) in 10 mM Tris, 150 mM NaCl, 0.5% Tween 20. The membranes were incubated with antibodies to Bax, Bcl-2, COX IV (1:1000; Santa Cruz Biotechnology); cytochrome *c* (1:1000; Cell Signaling Technology); UCP3 (1:1000; US Biological); MAO-A, peroxiredoxin 3 and 5 (1:1000; Abcam); or glyceraldehyde-3-phosphate dehydrogenase (GAPDH; 1:1000; Sigma). followed by the appropriate horseradish peroxidase-conjugated secondary antibodies and visualized by an enhanced chemiluminescence (Pierce) detection system. Protein levels were normalized to that of GAPDH.

For detection of cytochrome *c* release from mitochondria to cytosol, protein extraction of the cytosolic fractions was performed using a method as described previously with slight modifications [24]. Briefly, heart tissue was homogenized by gently douncing 30 times in a glass Dounce homogenizer in 7 volumes of cold suspension buffer A (20 mM HEPES–KOH, pH 7.5, 250 mM sucrose, 10 mM KCl, 1.5 mM $MgCl_2$, 1 mM EDTA, 1 mM EGTA, 1 mM DTT, 17 μg/ml phenylmethanesulfonyl fluoride, 2 μg/ml leupeptin, 8 μg/ml aprotinin). Unlysed tissue and nuclei were pelleted via a 10-min, 750 *g* spin. The supernatant was centrifuged at 10,000*g* for 25 min. This pellet was resuspended in buffer A and represents the mitochondrial fraction. The supernatant was centrifuged at 100,000*g* for 1 h at 4 °C. The supernatant from this final centrifugation represents the soluble cytosolic fraction. We examined possible cross-contamination by COX subunit IV as a mitochondrial and GAPDH as a cytosolic marker in both fractions.

1.13. Statistical analysis

Data are presented as the mean ± SEM. Comparison between groups was performed by one-way ANOVA, followed by a Tukey's post hoc multiple comparison test, and comparisons between two groups were performed using unpaired two-tailed Student *t* test using Prism 4.0 GraphPad software (GraphPad, San Diego, CA, USA). A value of $p < 0.05$ was considered significant.

2. Results

2.1. General effects of clorgyline on diabetic and control rats

STZ-administered rats showed characteristic symptoms of diabetes, including polydipsia, polyuria, and increased food intake, along with reduced body weight. Moreover, heart-to-body weight ratio (HW/BW) in the STZ group was higher than in the vehicle control group ($p < 0.01$). STZ-induced diabetes led to a decrease in the serum insulin levels ($p < 0.01$) with concomitant increase in blood glucose levels ($p < 0.001$).

After 8 weeks of diabetes, the STZ groups showed significantly

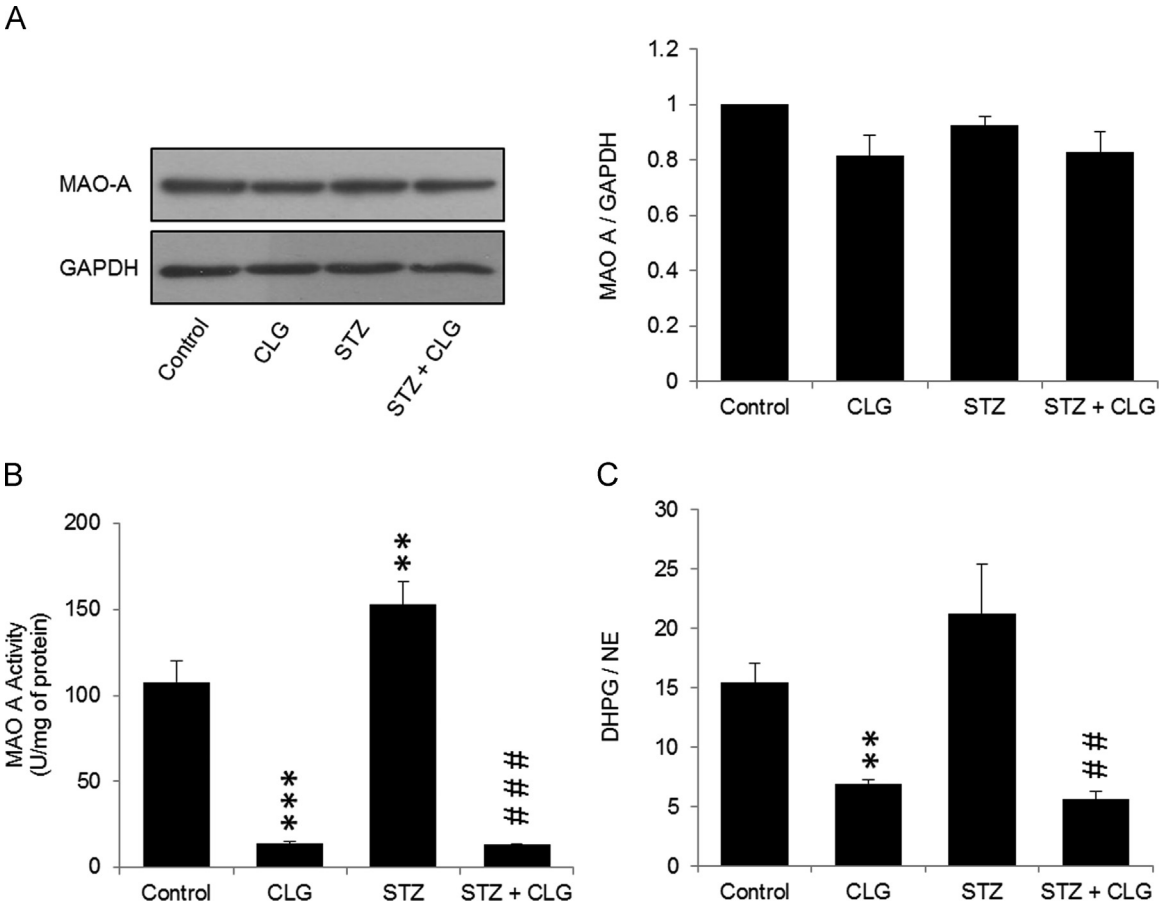

Fig. 2. Diabetes induces myocardial MAO-A activity. (A) MAO-A protein expression. Representative Western blot image (left) and densitometric analysis (right; $n = 8$/group). (B) MAO-A activity ($n = 6$–8/group) and (C) quantification of DHPG/NE ratio by HPLC method ($n = 4$/group). All values are given as the mean ± SE; $^{**}p < 0.01$, $^{***}p < 0.001$ vs control group; $^{\#\#}p < 0.01$, $^{\#\#\#}p < 0.001$ vs STZ group.

higher levels of total cholesterol than the vehicle control groups ($p < 0.001$) and exhibited lower HDL/LDL ratio than the vehicle control groups ($p < 0.05$). Serum biomarkers of liver damage, SGPT and SGOT, were higher in diabetic rats compared to vehicle control rats ($p < 0.05$). However, CLG treatment did not alter any of these parameters. Serum levels of troponin I, the biomarker of cardiac damage, showed significant increase in diabetic rats ($p < 0.001$) and was restored to normal by CLG treatment ($p < 0.05$) (Table 1).

2.2. MAO-A inhibition restored cardiac dysfunction assessed by electrocardiography and catheterization

ECG analysis was performed to investigate the changes in electrical activity of the heart. At 8 weeks after the induction of diabetes, slower heart rate was evident in diabetic rats compared to vehicle control rats ($p < 0.05$). Compared to vehicle control, diabetic rats showed prolongation of QRS interval ($p < 0.001$), QT interval ($p < 0.01$), and QTc interval ($p < 0.05$), indicating development of intraventricular conduction abnormalities. To further confirm the LV dysfunction, MABP, LVSP, LVEDP, contractility index, systolic and diastolic durations were measured by cardiac catheterization. Compared to vehicle controls, diabetic rats showed increase in MABP ($p < 0.05$), systolic duration ($p < 0.01$), and diastolic duration ($p < 0.05$). These changes were normalized with CLG administration. Diabetic condition also caused significant reduction in contractility index ($p < 0.05$) (Table 2). Compared to vehicle control, diabetic rats showed increases in LVSP ($p < 0.05$) and LVEDP ($p < 0.05$), whereas $(-dp/dt_{min})$/LVSP was decreased (Fig. 1). However; CLG treatment restored each of these parameters to normal.

2.3. MAO-A inhibition attenuates diabetes-induced oxidative stress

Diabetes did not alter the expression of myocardial MAO-A protein (Fig. 2A). However, a significant increase in MAO-A activity was observed in the myocardium of diabetic rats ($p < 0.01$) (Fig. 2B). Further we assessed cardiac levels of the MAO-A substrate NE and its catabolic product DHPG. Higher DHPG/NE ratio confirms increased MAO-A activity in the heart of diabetic rats compared to vehicle control rats (Fig. 2C). CLG treatment showed 90% reduction ($p < 0.001$) in MAO-A activity without altering its protein expression.

Further, we examined the relationship between MAO-A and cardiac oxidative stress in the STZ-induced diabetic rats. Lipid peroxidation, a major marker of oxidative stress, was assessed by examining cardiac levels of 4-HNE and MDA. Diabetic rats exhibited higher levels of myocardial 4-HNE than the vehicle control group ($p < 0.01$) and were restored to normal by CLG treatment ($p < 0.01$) (Fig. 3A). HPLC analysis showed that MDA levels were increased in myocardium of diabetic rats compared to vehicle controls and this increase was significantly reduced by CLG administration ($p < 0.05$) (Fig. 3B).

We next measured the activity of the antioxidant enzyme SOD in cardiac tissues of control and diabetic rats. An increase in the SOD activity was observed in the STZ group compared to the

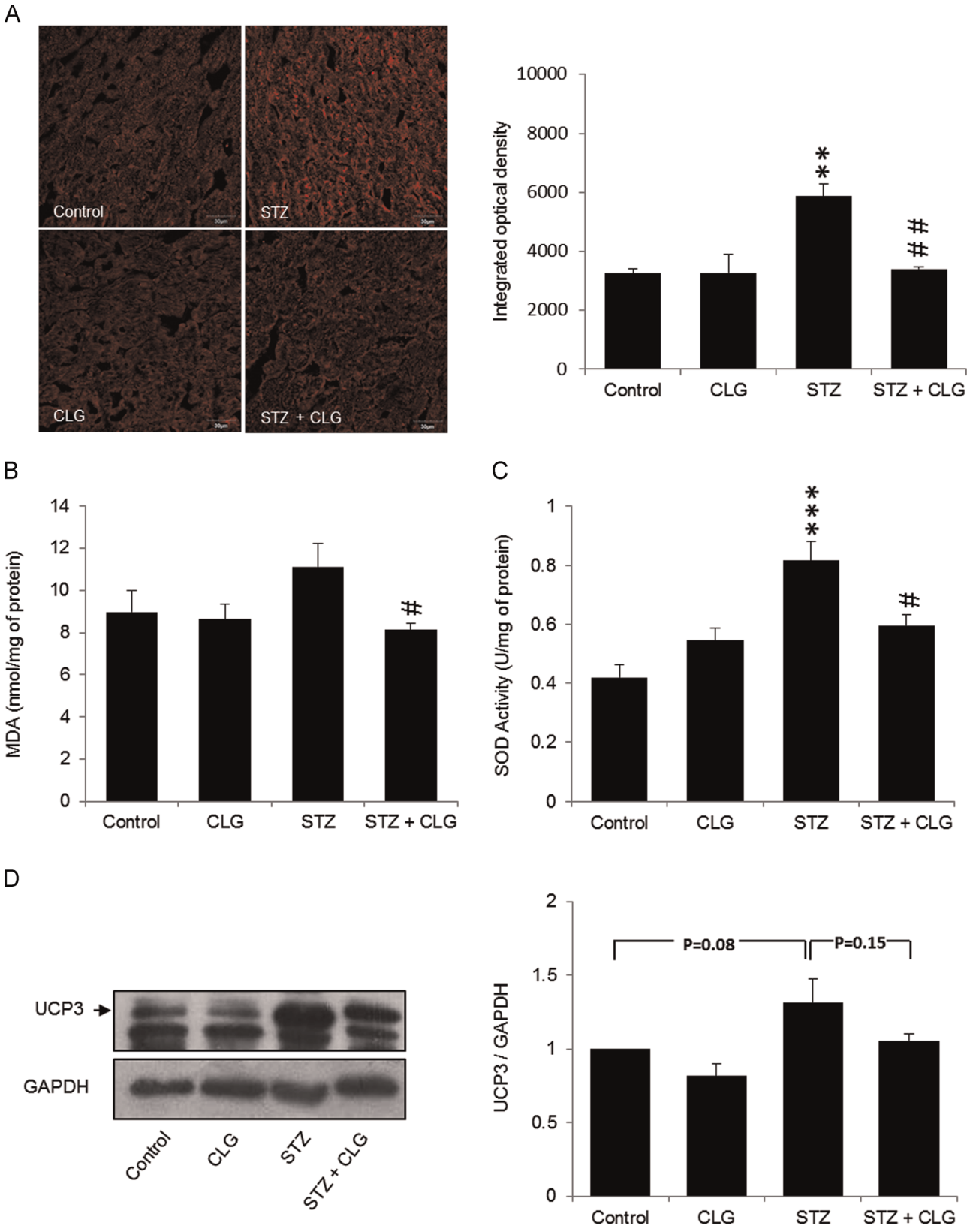

Fig. 3. MAO-A inhibition limits diabetes-induced myocardial oxidative stress. (A) (Left) Immunofluorescence staining for 4-HNE and (right) quantification of integrated optical density ($n = 4$/group). (B) Quantification of myocardial MDA levels by HPLC method ($n = 3$/group). (C) SOD activity ($n = 5$–9/group) and (D) UCP3 protein expression ($n = 5$/group). All values are given as the mean ± SE; $^{**}p < 0.01$, $^{***}p < 0.001$ vs control group; $^{\#}p < 0.05$, $^{\#\#}p < 0.01$ vs STZ group.

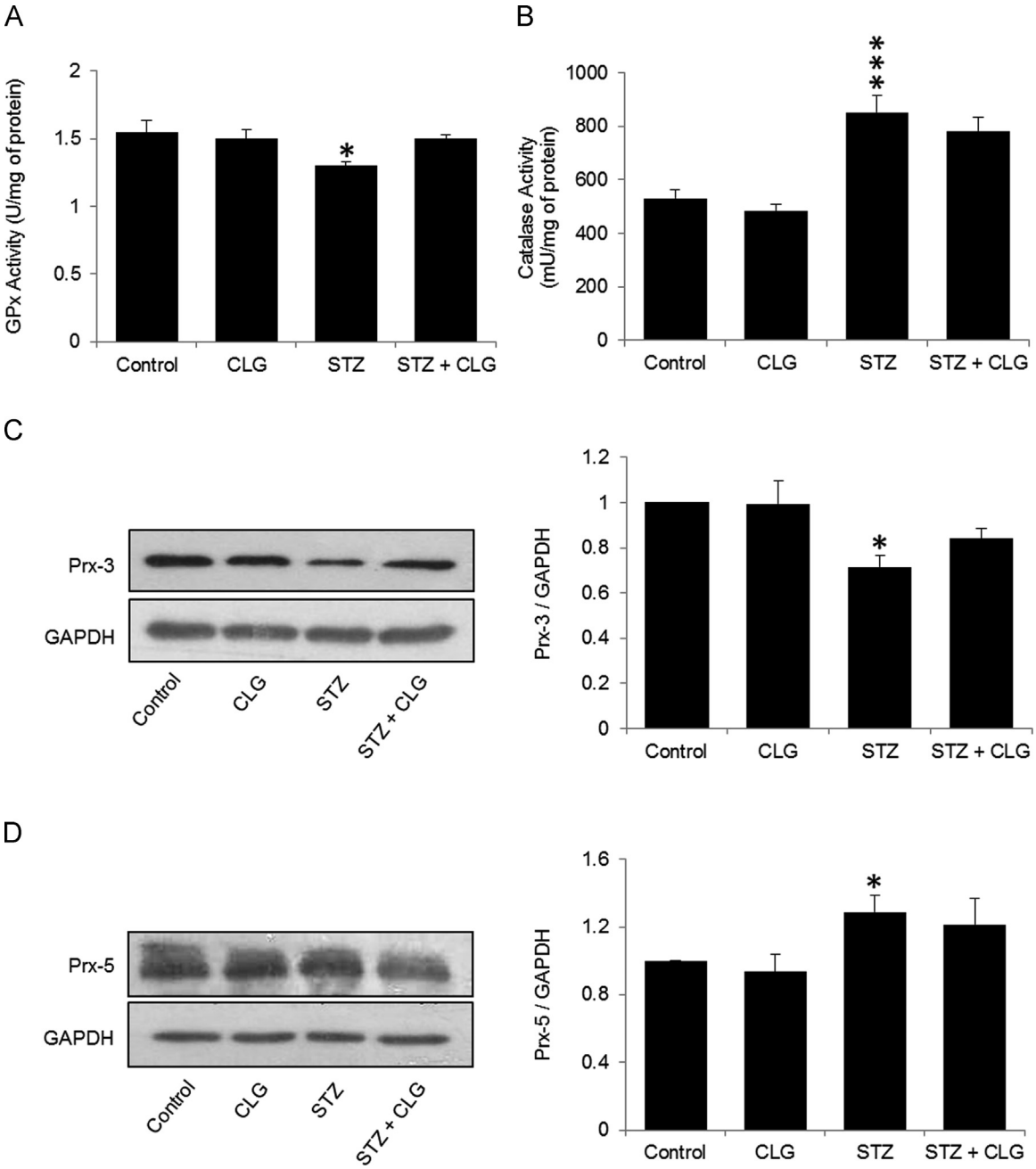

Fig. 4. Clorgyline treatment has no effect on myocardial H_2O_2-scavenging proteins. (A) Glutathione peroxidase (GPx) activity ($n = 5$/group). (B) Catalase activity ($n = 6$–9/group). (C) Peroxiredoxin-3 (Prx-3) protein expression. Representative Western blot image (left) and densitometric analysis (right; $n = 5$/group). (D) Prx-5 protein expression. Representative Western blot image (left) and densitometric analysis (right; $n = 6$/group). All values are given as the mean ± SE; $^{*}p < 0.05$, $^{***}p < 0.001$ vs control group.

vehicle control group ($p < 0.001$). This increase in SOD activity, which may be a compensatory response to the oxidative stress, was also reduced in diabetic rats treated with the CLG ($p < 0.05$) (Fig. 3C). We also observed a remarkable increase in myocardial UCP3 protein expression, a marker of mitochondrial uncoupling and redox stress, in the diabetic group, and CLG treatment was able to restore the protein levels of UCP3 to normal (Fig. 3D).

Because the antioxidant enzymes catalase, GPx, peroxiredoxin-3 (Prx-3), and peroxiredoxin-5 (Prx-5) are known to specifically scavenge H_2O_2 in cytoplasm and mitochondria, we further measured the activity of catalase and GPx and examined the protein expression of Prx-3 and Prx-5. We observed a decrease in the GPx activity (Fig. 4A) and Prx-3 protein expression (Fig. 4C) and an increase in the catalase activity (Fig. 4B) and Prx-5 protein expression (Fig. 4D) in hearts of STZ-induced diabetic rats. However, CLG treatment had no effect on these alterations.

2.4. MAO-A inhibition prevents cardiac apoptosis

We investigated the role of MAO-A in the molecular mechanisms involved in diabetes-induced cardiac apoptosis. In particular, we focused on the expression of Bcl-2 and Bax proteins. Bcl-2 and Bax are homologous proteins that have opposing effects on cell survival and death, with Bcl-2 serving to prolong cell survival and Bax acting as an accelerator of apoptosis [25]. Thus the Bcl-2/Bax ratio serves as one of the important markers of apoptosis. We examined the expression of Bcl-2 and Bax by Western blotting. Diabetic rats showed significant decrease ($p < 0.05$) in Bcl-2/Bax

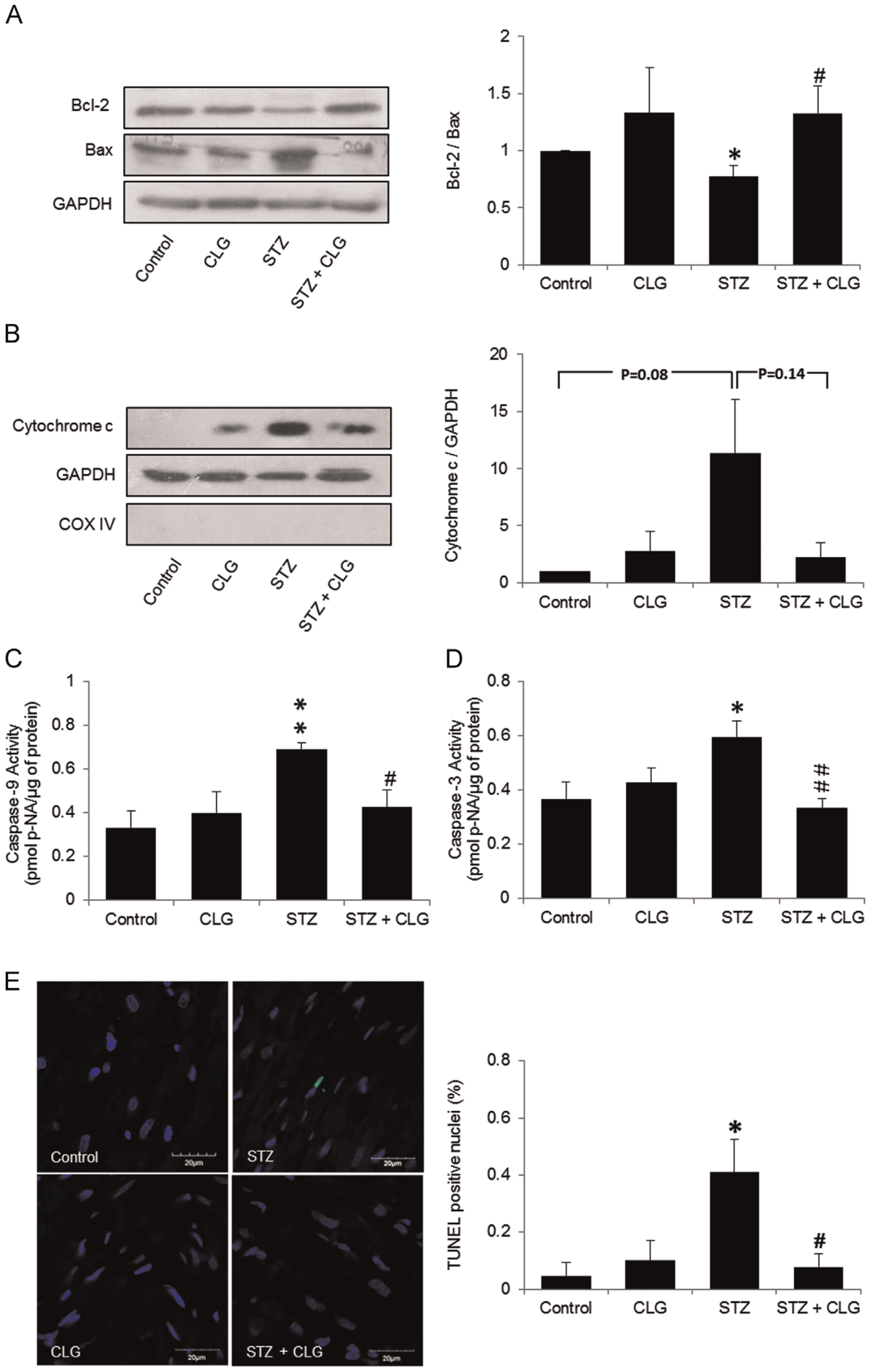

Fig. 5. MAO-A inhibition prevents diabetes-induced myocardial apoptosis. (A) Bcl-2 and Bax protein expression. Representative western blot image (left) and quantification (right, $n = 7$/group). (B) Analysis of cytosolic cytochrome *c* levels. Representative Western blot image (left) and quantification (right; $n = 3$/group). (C) Caspase 9 activity ($n = 4$–7/group). (D) Caspase 3 activity ($n = 5$ or 6/group). (E) Examination of cardiac apoptosis using TUNEL staining. Representative TUNEL section shown on left, arrow indicates TUNEL-positive nucleus, and quantification (right; $n = 3$ or 4/group). All values are given as the mean ± SE; $^{*}p < 0.05$, $^{**}p < 0.01$ vs control group; $^{\#}p < 0.05$, $^{\#\#}p < 0.01$ vs STZ group.

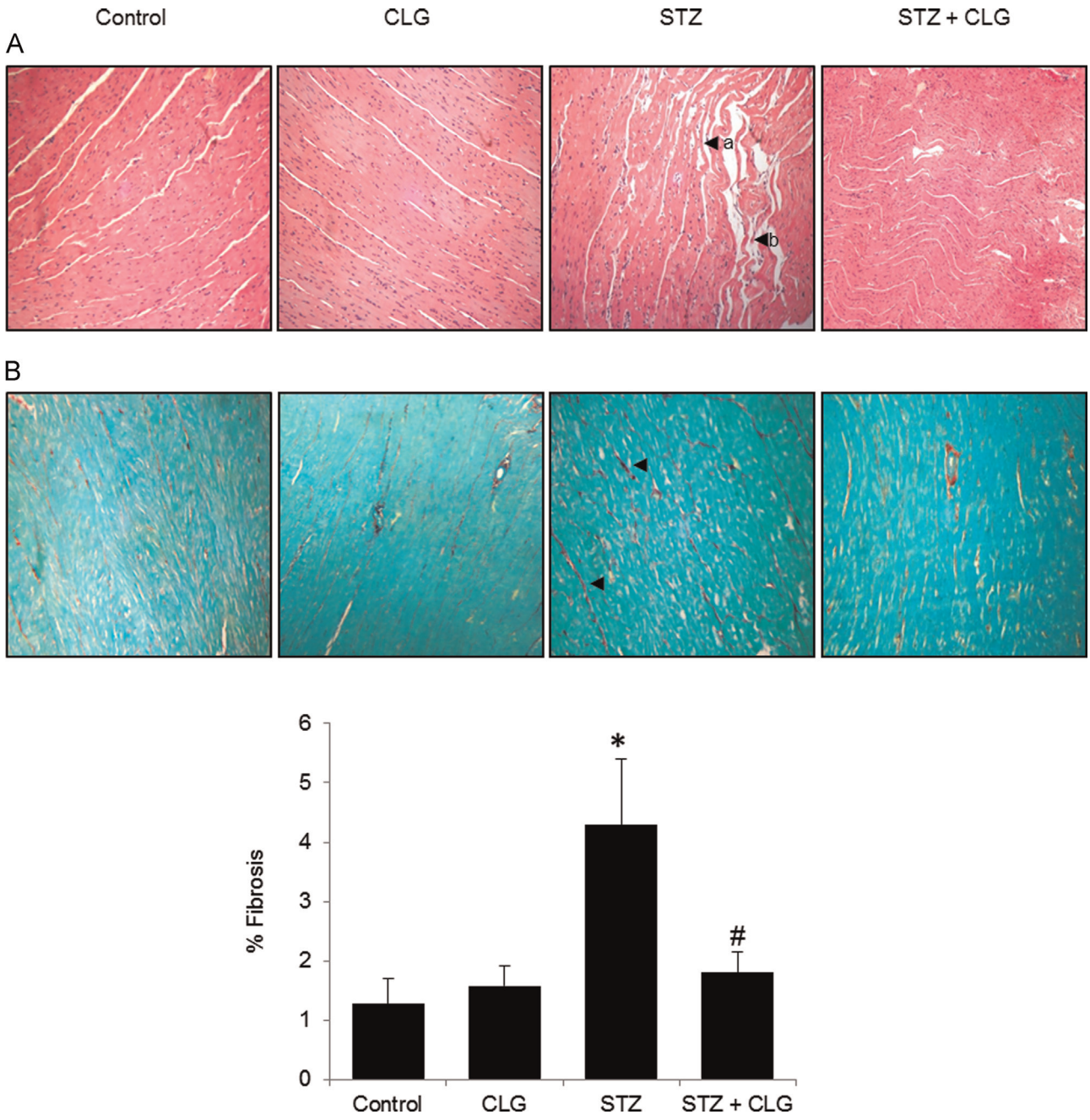

Fig. 6. MAO-A inhibition attenuates diabetes-induced changes in myocardial histology and cardiac fibrosis. (A) Representative H&E-stained cardiac sections; arrows demonstrate (a) separation and (b) degeneration of myocardial fibers. (B) Cardiac fibrosis. Representative Sirius red-stained sections (above), collagen appears red as indicated by arrows, and quantification (below; $n = 5$/group). All values are given as the mean $\pm$ SE; $^{*}p < 0.05$ vs control group; $^{\#}p < 0.05$ vs STZ group.

ratio compared to controls. Interestingly, after treatment with CLG, Bcl-2 and Bax levels were seen to be normalized, resulting in a significantly increased Bcl-2/Bax ratio ($p < 0.05$) (Fig. 5A).

Previous reports revealed that Bax induces the release of cytochrome *c* from mitochondria to cytoplasm, whereas Bcl-2 prevents it [26,27]. Further, it is reported that caspases are important regulators of apoptosis, and the release of cytochrome *c* from mitochondria activates caspases, especially caspase 3 [28]. Therefore, we analyzed the effect of MAO-A inhibition on release of cytochrome *c* and activation of caspases implicated in cardiac cell death.

To detect cytochrome *c* release, subcellular fractionation of heart tissues followed by Western blot analysis of cytosolic fraction was carried out. Results showed that cytosolic cytochrome *c* levels were increased in the diabetic group compared to vehicle control ($p = 0.07$ by one-way ANOVA) (Fig. 5B). Moreover heart of diabetic rat showed significant increase in the activities of caspase 9 ($p < 0.01$) (Fig. 5C) and caspase 3 ($p < 0.05$) (Fig. 5D) compared to vehicle controls. CLG treatment significantly reduced all these adverse phenomena.

In the vehicle control rat hearts, TUNEL-positive nuclei were seldom identified, but in diabetic rat hearts, numerous TUNEL-positive nuclei were observed ($p < 0.05$). Diabetic rats treated with CLG showed a significant reduction in the number of TUNEL-positive nuclei compared to untreated diabetic rat ($p < 0.05$) (Fig. 5E).

2.5. Diabetes-induced myocardial morphological changes and cardiac fibrosis are ameliorated by treatment with clorgyline

H&E staining of the heart tissues showed that, compared with vehicle control, diabetic hearts displayed structural abnormalities such as degeneration of cardiac myofibrils, a marked separation of myocardial fibers from one another, congestion and hemorrhages in epicardium, and accumulation of polymorphonuclear neutrophils. However, structural abnormalities in the hearts of diabetic rats were prevented by CLG treatment (Fig. 6A).

Myocardial fibrosis was examined by Sirius red staining. Diabetes induced a significant increase ($p < 0.05$) in myocardial interstitial and perivascular collagen deposition compared to vehicle control. The fibrotic changes in the heart were significantly alleviated when diabetic rats were treated with CLG (Fig. 6B).

3. Discussion

In the current study, we demonstrated that pharmacological inhibition of MAO-A restored cardiac dysfunction in an animal model of type I diabetes. This was accompanied by decreased cardiac oxidative stress, apoptosis, and fibrosis. All these beneficial effects of MAO-A inhibition were seen despite persistent hyperglycemia and hyperlipidemia, thus excluding the possibility of potential cardioprotective effects due to clorgyline-elicited global metabolic benefits.

MAOs are important sources of ROS in the heart and MAO-A-derived ROS play a deleterious role under cardiac duress such as hearts subjected to hemodynamic overload or I/R injury [9,10]. In the present study we found that MAO-A activity increases in the hearts of STZ-induced diabetic rats and administration of the MAO-A-specific inhibitor CLG prevented diabetes-induced oxidative stress. We might predict that the reduction in oxidative stress is due to inhibition of MAO-A-mediated H_2O_2 production, as we have excluded the involvement of other H_2O_2 scavengers such as catalase, glutathione peroxidase, and peroxiredoxins.

Increased levels of ROS are documented to have a causative effect on diabetic cardiomyopathy [29,30]. A previous report has shown that in STZ-induced diabetic rats, ROS leads to cardiac cell death via a mitochondria-dependent apoptotic pathway [24]. Consistent with this report we observed myocardial apoptosis in the STZ-induced diabetic rats as evidenced by decreased Bcl-2/Bax ratio, cytochrome *c* release, activation of the caspase cascade, and increased TUNEL-positive nuclei. These observations could be reversed by MAO-A inhibition, indicating that MAO-A-derived ROS trigger myocardial apoptosis via an intrinsic pathway.

Diastolic dysfunction is one of the earliest manifestations in the progression of diabetic cardiomyopathy [31, 32]. $-dp/dt$, a cardiac diastolic index, is widely used to assess diastolic function. Because LVSP was demonstrated to be a hemodynamic determinant of $-dp/dt_{min}$, several studies have implemented $(-dp/dt_{min})$/LVSP to evaluate left-ventricular diastolic function more accurately [33–36]. Thus we selected both $-dp/dt_{min}$ and $(-dp/dt_{min})$/LVSP to determine whether MAO-A inhibition could restore diastolic function in diabetic rats. STZ-induced diabetic rats developed diastolic dysfunction as indicated by a significant increase in LVEDP and reduced $(-dp/dt_{min})$/LVSP. MAO-A inhibition in turn restored each of these parameters. Additionally, cardiac fibrosis has been correlated with diastolic dysfunction [37]. This is in agreement with our findings concerning impaired diastolic function, as was shown in the current study by invasive LVP data. In STZ-induced diabetic rats, an elevation in myocardial collagen content was prevented by CLG treatment. This further supports a beneficial effect of MAO-A inhibition in preventing excess accumulation of extracellular matrix proteins, which may impede LV contractility. Diabetes also affects electrical activity of the heart and ECG offers a noninvasive screen to assess these changes [38,39]. QTc interval, an electrocardiographic parameter, is of particular clinical significance as it is a prominent predictor of stroke and mortality in patients with diabetes [40,41]. In our model of type I diabetes, ECG showed QTc prolongation, an observation that is consistent with previous work [39,42]. CLG treatment significantly reduced this QTc dispersion. All these observations indicate that increased MAO-A activity contributes to the development of cardiac contractile dysfunction in diabetic cardiomyopathy.

4. Conclusions

In summary our findings support MAO-A as an important source of ROS that contribute to oxidative stress in DCM. Furthermore, prevention of cardiac contractile dysfunction, apoptosis, and fibrosis by a specific inhibitor of MAO-A, clorgyline, suggests that an increase in cardiac MAO-A activity could play a major role in the progression of DCM and proposes MAO-A as a promising pharmaceutical target for cardioprotection in diabetes.

Authors' contributions

P.U. and S.L.S. contributed to the design of the study, data analysis, and interpretation of results. P.U., S.S., S.A., N.V., and S.L. contributed to data acquisition. P.U., S.L.S., and S.S. contributed to drafting of the manuscript.

Acknowledgement

The authors thank Nikhila Vengala (Department of Pharmacology, Poona College of Pharmacy, Pune, India) for help with hemodynamic and electrocardiographic assessment of rat cardiac function. We thank Aparajita Dasgupta for proofreading the manuscript. We also acknowledge the help from the staff of the experimental animal facility at the National Centre for Cell Science. This work was supported by the National Centre for Cell Science, Department of Biotechnology, and India. P.U. (Sr. No. 2061030917), S.S. (Sr. No. 2061030712), and S.A. (Sr. No. 2061030780) are recipients of University Grants Commission Senior Research Fellowships.

References

[1] I.G. Poornima, P. Parikh, R.P. Shannon, Diabetic cardiomyopathy: the search for a unifying hypothesis, Circ. Res. 98 (2006) 596–605.
[2] B. Swynghedauw, Molecular mechanisms of myocardial remodeling, Physiol. Rev. 79 (1999) 215–262.
[3] J.W. Baynes, Role of oxidative stress in development of complications in diabetes, Diabetes 40 (1991) 405–412.
[4] Y. Chen, J.T. Saari, Y.J. Kang, Weak antioxidant defenses make the heart a target for damage in copper-deficient rats, Free Radic. Biol. Med. 17 (1994) 529–536.
[5] S. Kumar, S. Prasad, S.L. Sitasawad, Multiple antioxidants improve cardiac complications and inhibit cardiac cell death in streptozotocin-induced diabetic rats, PLoS One 8 (2013) e67009.
[6] Z. Guo, Z. Xia, J. Jiang, J.H. McNeill, Downregulation of NADPH oxidase, antioxidant enzymes, and inflammatory markers in the heart of streptozotocin-induced diabetic rats by N-acetyl-L-cysteine, Am. J. Physiol. Heart Circ. Physiol 292 (2007) H1728–H1736.
[7] L. Cai, Y. Wang, G. Zhou, T. Chen, Y. Song, X. Li, et al., Attenuation by metallothionein of early cardiac cell death via suppression of mitochondrial oxidative stress results in a prevention of diabetic cardiomyopathy, J. Am. Coll. Cardiol. 48 (2006) 1688–1697.
[8] P. Rosen, T. Ballhausen, W. Bloch, K. Addicks, Endothelial relaxation is disturbed by oxidative stress in the diabetic rat heart: influence of tocopherol as

antioxidant, Diabetologia 38 (1995) 1157–1168.
[9] N. Kaludercic, A. Carpi, R. Menabo, L.F. Di, N. Paolocci, Monoamine oxidases (MAO) in the pathogenesis of heart failure and ischemia/reperfusion injury, Biochim. Biophys. Acta 1813 (2011) 1323–1332.
[10] N. Kaludercic, E. Takimoto, T. Nagayama, N. Feng, E.W. Lai, D. Bedja, et al., Monoamine oxidase A-mediated enhanced catabolism of norepinephrine contributes to adverse remodeling and pump failure in hearts with pressure overload, Circ. Res. 106 (2010) 193–202.
[11] C. Villeneuve, C. Guilbeau-Frugier, P. Sicard, O. Lairez, C. Ordener, T. Duparc, et al., p53-PGC-1alpha pathway mediates oxidative mitochondrial damage and cardiomyocyte necrosis induced by monoamine oxidase-A upregulation: role in chronic left ventricular dysfunction in mice, Antioxid. Redox Signaling 18 (2013) 5–18.
[12] A. Carpi, R. Menabo, N. Kaludercic, P. Pelicci, L.F. Di, M. Giorgio, The cardioprotective effects elicited by p66 (Shc) ablation demonstrate the crucial role of mitochondrial ROS formation in ischemia/reperfusion injury, Biochim. Biophys. Acta 1787 (2009) 774–780.
[13] P. Bianchi, O. Kunduzova, E. Masini, C. Cambon, D. Bani, L. Raimondi, et al., Oxidative stress by monoamine oxidase mediates receptor-independent cardiomyocyte apoptosis by serotonin and post ischemic myocardial injury, Circulation 112 (2005) 3297–3305.
[14] D. Pchejetski, O. Kunduzova, A. Dayon, D. Calise, M.H. Seguelas, N. Leducq, et al., Oxidative stress-dependent sphingosine kinase-1 inhibition mediates monoamine oxidase A-associated cardiac cell apoptosis, Circ. Res. 100 (2007) 41–49.
[15] C.A. Maggi, A. Meli, Suitability of urethane anesthesia for physiopharmacological investigations in various systems. Part 2. Cardiovascular system, Experientia 42 (1986) 292–297.
[16] K.S. Heffernan, S.Y. Jae, B. Fernhall, Heart rate recovery after exercise is associated with resting QTc interval in young men, Clin. Auton. Res. 17 (2007) 356–363.
[17] Y.K. Gupta, M. Sharma, G. Chaudhary, Pyrogallol-induced hepatotoxicity in rats: a model to evaluate antioxidant hepatoprotective agents, Methods Find. Exp. Clin. Pharmacol. 24 (2002) 497–500.
[18] D. Grotto, L.D. Santa Maria, S. Boeira, J. Valentini, M.F. Charao, A.M. Moro, et al., Rapid quantification of malondialdehyde in plasma by high performance liquid chromatography-visible detection, J. Pharm. Biomed. Anal. 43 (2007) 619–624.
[19] M.K. Lakshmana, T.R. Raju, An isocratic assay for norepinephrine, dopamine, and 5-hydroxytryptamine using their native fluorescence by high-performance liquid chromatography with fluorescence detection in discrete brain areas of rat, Anal. Biochem. 246 (1997) 166–170.
[20] M. Zhou, N. Panchuk-Voloshina, A one-step fluorometric method for the continuous measurement of monoamine oxidase activity, Anal. Biochem. 253 (1997) 169–174.
[21] J.P. Jacobsen, W.B. Siesser, B.D. Sachs, S. Peterson, M.J. Cools, V. Setola, et al., Deficient serotonin neurotransmission and depression-like serotonin biomarker alterations in tryptophan hydroxylase 2 (Tph2) loss-of-function mice, Mol. Psychiatry 17 (2012) 694–704.
[22] Y. Zhang, S.A. Babcock, N. Hu, J.R. Maris, H. Wang, J. Ren, Mitochondrial aldehyde dehydrogenase (ALDH2) protects against streptozotocin-induced diabetic cardiomyopathy: role of GSK3beta and mitochondrial function, BMC Med. 10 (2012) 40.
[23] G. Zhou, X. Li, D.W. Hein, X. Xiang, J.P. Marshall, S.D. Prabhu, et al., Metallothionein suppresses angiotensin II-induced nicotinamide adenine dinucleotide phosphate oxidase activation, nitrosative stress, apoptosis, and pathological remodeling in the diabetic heart, J. Am. Coll. Cardiol. 52 (2008) 655–666.
[24] L. Cai, W. Li, G. Wang, L. Guo, Y. Jiang, Y.J. Kang, Hyperglycemia-induced apoptosis in mouse myocardium: mitochondrial cytochrome C-mediated caspase-3 activation pathway, Diabetes 51 (2002) 1938–1948.
[25] J.C. Reed, Bcl-2 and the regulation of programmed cell death, J. Cell Biol. 124 (1994) 1–6.
[26] R.M. Kluck, E. Bossy-Wetzel, D.R. Green, D.D. Newmeyer, The release of cytochrome c from mitochondria: a primary site for Bcl-2 regulation of apoptosis, Science 275 (1997) 1132–1136.
[27] J. Yang, X. Liu, K. Bhalla, C.N. Kim, A.M. Ibrado, J. Cai, et al., Prevention of apoptosis by Bcl-2: release of cytochrome c from mitochondria blocked, Science 275 (1997) 1129–1132.
[28] D.R. Green, J.C. Reed, Mitochondria and apoptosis, Science 281 (1998) 1309–1312.
[29] L. Cai, Y.J. Kang, Oxidative stress and diabetic cardiomyopathy: a brief review, Cardiovasc. Toxicol. 1 (2001) 181–193.
[30] Z.V. Varga, Z. Giricz, L. Liaudet, G. Hasko, P. Ferdinandy, P. Pacher, Interplay of oxidative, nitrosative/nitrative stress, inflammation, cell death and autophagy in diabetic cardiomyopathy, Biochim. Biophys. Acta 1852 (2015) 232–242.
[31] D.C. Raev, Which left ventricular function is impaired earlier in the evolution of diabetic cardiomyopathy? An echocardiographic study of young type I diabetic patients, Diabetes Care 17 (1994) 633–639.
[32] C.M. Schannwell, M. Schneppenheim, S. Perings, G. Plehn, B.E. Strauer, Left ventricular diastolic dysfunction as an early manifestation of diabetic cardiomyopathy, Cardiology 98 (2002) 33–39.
[33] M.L. Weisfeldt, H.E. Scully, J. Frederiksen, J.J. Rubenstein, G.M. Pohost, E. Beierholm, et al., Hemodynamic determinants of maximum negative dP-dt and periods of diastole, Am. J. Physiol. 227 (1974) 613–621.
[34] M. Slama, J. Ahn, M. Peltier, J. Maizel, D. Chemla, J. Varagic, et al., Validation of echocardiographic and Doppler indexes of left ventricular relaxation in adult hypertensive and normotensive rats, Am. J. Physiol. Heart Circ. Physiol 289 (2005) H1131–H1136.
[35] C. Grousset, P. Menasche, C.S. Apstein, C. Mouas, F. Marotte, A. Piwnica, Protective effects of cardioplegia on diastolic function of hypertrophied rat hearts after hypothermic ischaemic arrest, Eur. Heart J. 5 (Suppl. F) (1984) 347–353.
[36] T. Ogata, T. Miyauchi, S. Sakai, M. Takanashi, Y. Irukayama-Tomobe, I. Yamaguchi, Myocardial fibrosis and diastolic dysfunction in deoxycorticosterone acetate-salt hypertensive rats is ameliorated by the peroxisome proliferator-activated receptor-alpha activator fenofibrate, partly by suppressing inflammatory responses associated with the nuclear factor-kappa-B pathway, J. Am. Coll. Cardiol. 43 (2004) 1481–1488.
[37] K. Mizushige, L. Yao, T. Noma, H. Kiyomoto, Y. Yu, N. Hosomi, K. Ohmori, H. Matsuo, Alteration in left ventricular diastolic filling and accumulation of myocardial collagen at insulin-resistant prediabetic stage of a type II diabetic rat model, Circulation 101 (2000) 899–907.
[38] S. Stern, S. Sclarowsky, The ECG in diabetes mellitus, Circulation 120 (2009) 1633–1636.
[39] F.C. Howarth, M. Jacobson, O. Naseer, E. Adeghate, Short-term effects of streptozotocin-induced diabetes on the electrocardiogram, physical activity and body temperature in rats, Exp. Physiol. 90 (2005) 237–245.
[40] P.K. Christensen, M.A. Gall, A. Major-Pedersen, A. Sato, P. Rossing, L. Breum, et al., QTc interval length and QT dispersion as predictors of mortality in patients with non-insulin-dependent diabetes, Scand. J. Clin. Lab. Invest. 60 (2000) 323–332.
[41] C.R. Cardoso, G.F. Salles, W. Deccache, QTc interval prolongation is a predictor of future strokes in patients with type 2 diabetes mellitus, Stroke 34 (2003) 2187–2194.
[42] S.L. Badole, G.B. Jangam, S.M. Chaudhari, A.E. Ghule, A.A. Zanwar, L-Glutamine supplementation prevents the development of experimental diabetic cardiomyopathy in streptozotocin-nicotinamide induced diabetic rats, PLoS One 9 (2014) e92697.